Dynamic Mechanical Properties of Short Carbon Fiber-Filled Styrene–Isoprene–Styrene Block Copolymer

D. ROY, A. K. BHOWMICK, and S. K. DE*

Rubber Technology Centre, Indian Institute of Technology, Kharagpur 721 302, India

SYNOPSIS

The mechanical and dynamic mechanical properties of short carbon fiber-filled styrene–isoprene–styrene (S–I–S) block thermoplastic elastomeric composite have been studied. Brabender mixing followed by milling of the fiber–rubber compositions caused about a 30-fold decrease in the fiber aspect ratio and random fiber orientation. Although low-strain moduli increased on fiber incorporation, tensile and tear properties dropped and anisotropy in mechanical properties was not observed. Tan δ values at the T_g region decreased on filler incorporation, but at room temperature, the tan δ values increased with filler loading. The variation of storage moduli and tan δ values with frequency followed a pattern similar to the variation of these properties with filler incorporation. © 1993 John Wiley & Sons, Inc.

INTRODUCTION

Short carbon fiber reinforcement in plastics has met with great success over the last few decades.[1–4] Lately, short fiber-reinforced rubber composites have become popular because of the advantages of high low-strain moduli, damping, stiffness, and processing advantages.[5–9] However, one great disadvantage of such composites is the problem of stress transfer between the hard fiber phase and the soft elastomeric phase. Thermoplastic elastomers offer novel opportunities in this area in the sense that hard domains in the morphology of these polymers may assist in effective stress transfer. However, short fiber reinforcement of thermoplastic elastomer has not received the desired attention. Akhtar et al.[10] reported processing and failure properties of a short silk fiber-filled thermoplastic elastomeric blend of natural rubber and polyethylene. Watson and Frances[11] studied thermoplastic rubber reinforced with Kevlar fiber for wear applications. The rheological behavior of short Kevlar fiber-filled thermoplastic polyurethane have been reported by Kutty et al.[12] Roy et al.[13] reported the mechanical and dynamic mechanical properties of short carbon fiber-filled thermoplastic elastomer based on a blend of natural rubber and high-density polyethylene. The viscoelastic properties of short fiber-filled rubber composites have also been reported.[14]

In the present work, we report the results of our studies on mechanical and dynamic mechanical properties of short carbon fiber-filled styrene–isoprene–styrene (S–I–S) thermoplastic rubber.

EXPERIMENTAL

Materials Used

Styrene–Isoprene–Styrene Block Copolymer

Kraton-D-1107, abbreviated as S–I–S, was obtained from Shell Development Co. The rubber has the following characteristics: specific gravity of 0.92 and styrene/isoprene ratio of 14/86.

Carbon Fiber

Grade RK-30 was obtained from RK Carbon Fibers Ltd., U.K. The fiber has the following characteristics: epoxy-treated; carbon content, 95% mass; density, 1.78 g/cc; tensile strength, 3.0 GPa; and tensile modulus, 220–240 GPa.

* To whom correspondence should be addressed.

Journal of Applied Polymer Science, Vol. 49, 263–273 (1993)
 CCC 0021-8995/93/020263-11

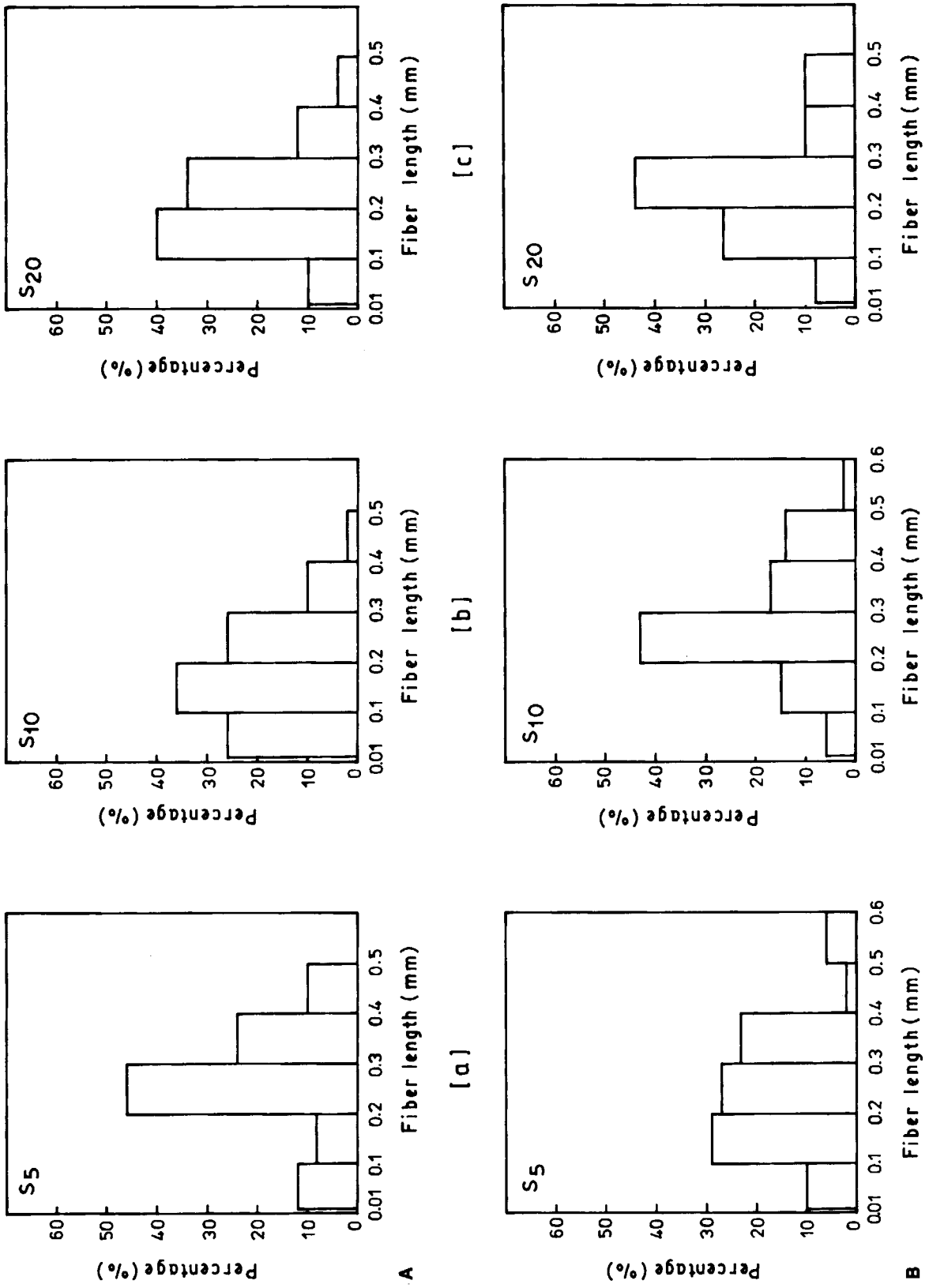

Figure 1 Histogram showing fiber-length distribution of Brabender mixed composition. (A) Before milling: (a) S_5; (b) S_{10}; (c) S_{20}. (B) After milling: (a) S_5; (b) S_{10}; (c) S_{20}.

Preparation of Fiber-Rubber Composites

Preparation of the Composite Based on S-I-S

Compositions of the mixes are given in Table I. The composites were prepared in a Brabender Plasticorder (Model PLE 330), using a cam-type rotor, with a speed of 50 rpm and the mixer chamber set at 150°C. Initially, the S-I-S was melted in the mixer for 2 min. Next, chopped carbon fiber (6 mm in length) was added to it and mixed for another 3 min. The mix was then taken out and sheeted through a laboratory mill with a nip setting of 2 mm. The sheeted material was then remixed in the plasticorder at 150°C for 2 min to ensure uniform dispersion of the fibers and homogeneity of the blend. Finally, the mix was sheeted out through the two-roll mill and compression-molded between two aluminum foils in a Toyoseiki Labo-Press at 170°C for 3 min. At the end of the molding time, the sample, still under compression, was cooled to room temperature by water circulation through the platens of the press.

Compositions without fibers were also molded under similar conditions. Mixing procedures of these compositions were the same as those described in the preceding paragraph.

Determination of Fiber Aspect Ratio

The fiber-filled composites were dissolved in benzene and the fibers were separated out after washing several times with benzene. The average length of the fibers was measured by a WILD Heerbrugg Optical Microscope, Model M3C TYP 325400, by taking more than 100 fibers. The diameter of the fibers in the composite was measured with Cam Scan Series II model scanning electron microscope (SEM).

Measurement of Mechanical and Dynamic Mechanical Properties

Measurement of modulus, tensile strength, and elongation at break was carried out at 25°C as per the ASTM D412-80 test method using dumbbell-shaped test pieces cut both in the longitudinal (along the milling) and transverse (across the milling) directions using a ZWICK Universal Testing Machine, Model 1445, at a cross-head speed of 500 mm/min. Tear strength of the samples was determined as per the ASTM D624-81 test method using unnicked 90° angle test pieces cut both in the longitudinal and transverse directions from the molded sheets. The hardness of the samples was measured by a Shore-A hardness tester.

Table I Formulations of the Composite[a]

Ingredients (phr)[b]	
S-I-S	100
Carbon fiber	0, 5, 10, 20

[a] Henceforth, S_0, S_5, S_{10}, and S_{20} would indicate the mixes containing 0, 5, 10, and 20 phr of fiber, respectively.
[b] phr means parts per 100 parts of rubber in grams.

The dynamic mechanical measurements such as the storage modulus (E') and the loss factor, tan δ, of the composites were performed with a computerized dynamic mechanical thermal analyzer, manufactured by Polymer Laboratories, U.K.,† which was operated in a bending mode with a fixed strain of 32 (peak-to-peak displacement in microns). The sample dimension was 40 × 12.5 × 1.74 mm. The frequencies used were 0.3, 1, 3, 10, and 30 Hz. The tests were performed in the temperature range of −100 to 70°C. Above 70°C, the sample became too soft to produce reliable results.

SEM Study

The SEM observations of the tensile failure surfaces of the fiber-filled composites were made on gold-coated samples using a Cam Scan Series II model scanning electron microscope.

RESULTS AND DISCUSSION

Fiber Aspect Ratio

The fiber aspect ratio dropped from an initial value (before Brabender mixing) of 880 to 30 after mixing. The high shearing force generated during Brabender mixing presumably exceeds the low bending strength of the fiber, causing considerable fiber breakage. The histogram showing the fiber length distribution (a) after Brabender mixing and (b) after milling of the Brabender mixed stock is shown in Figure 1. The average fiber lengths before and after being passed through the mill were 0.25 mm, 0.22 mm, 0.19 mm

† Polymer Laboratories Ltd., The Technology Centre, Epinal Way Loughborough, U.K., LE 11 OQE.

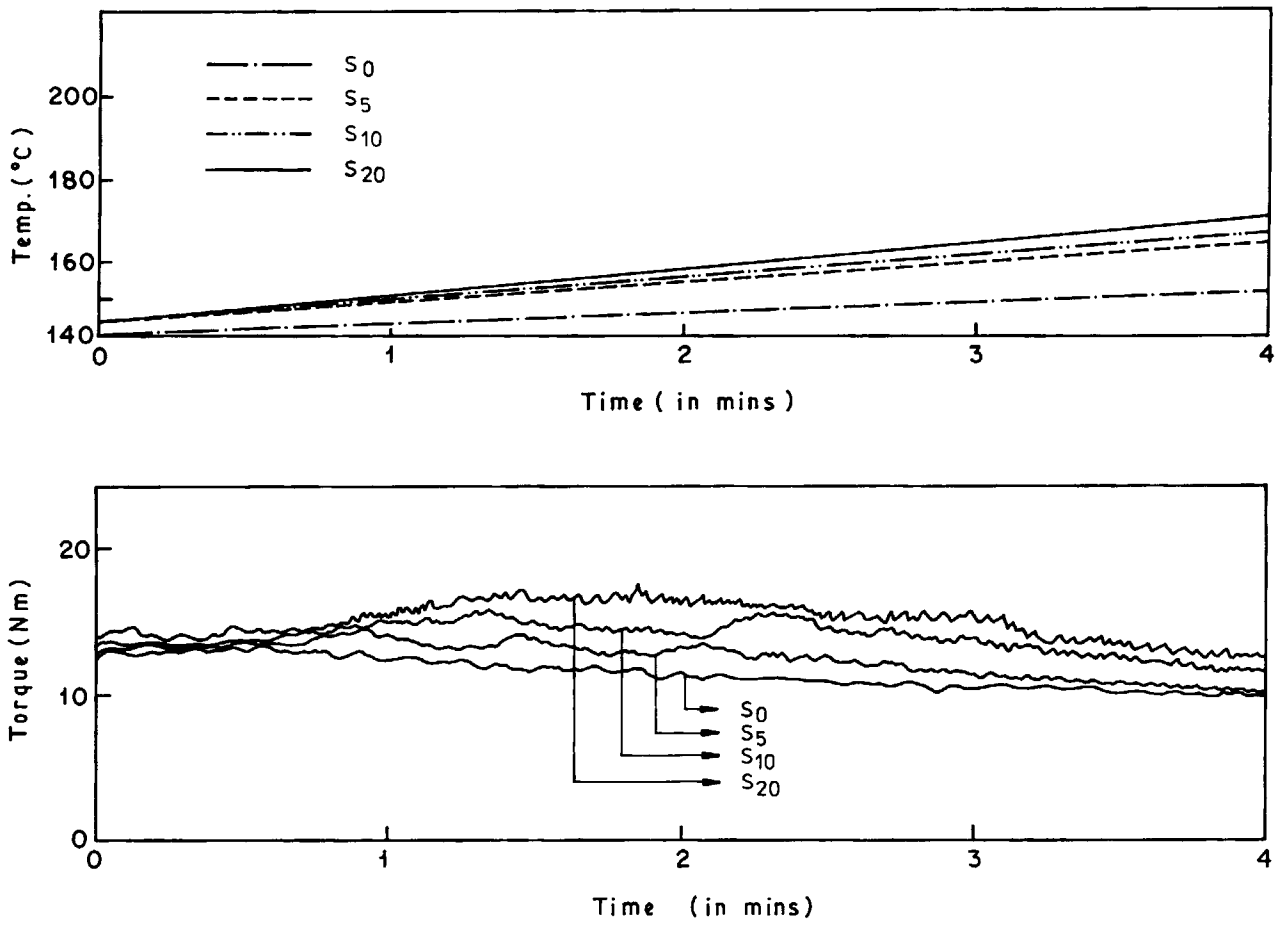

Figure 2 Variation of Brabender torque and temperature during mixing.

and 0.21 mm, 0.26 mm and 0.24 mm for 5, 10, and 20 phr carbon fiber in S–I–S, respectively. It is evident that the fiber aspect ratio is independent of the fiber concentration in the matrix and fiber breakage occurred mostly during the Brabender mixing operation. Both the torque and the temperature increased during mixing (Fig. 2). The results are summarized in Table II. It is observed that the torque increased with the increase of fiber concentration and the temperature also increased due to high shear generation in the plasticorder.

Fiber Orientation

Figure 3 shows the SEM fractograph of a fiber-filled S–I–S composite. It can be seen that fiber distribution is random in the polymer matrix. Furthermore, there is no difference in the stress–strain and tear strength between longitudinally and transversely oriented fiber composites (Table III). It has been shown earlier[15] that SEM fractography as well as low-strain moduli and failure properties are useful tools in determining fiber orientation in rubber composites.

Failure Properties

The effect of fiber incorporation on the stress–strain properties of S–I–S rubber is shown in Figure 4 and the results are summarized in Table III. It is evident that the low-strain moduli and hardness increased

Table II Brabender Torque and Temperature During Mixing

Mix No.	Fiber Loading (phr)	Maximum Torque (Nm)	Maximum Temperature (°C)
S_0	0	14	149
S_5	5	15	160
S_{10}	10	16	164
S_{20}	20	18	167

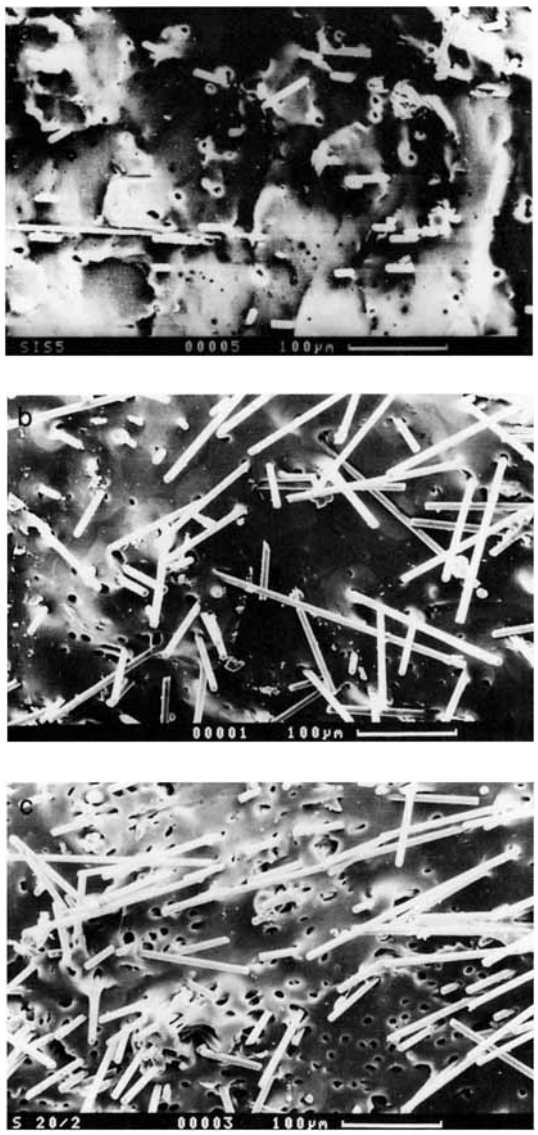

Figure 3 SEM photograph of the tensile fractured surface of the composites: (a) S_5; (b) S_{10}; (c) S_{20}.

and the tensile strength decreased with filler incorporation. The drop in tensile strength and the decrease in elongation at break along with the lowering of tear resistance on fiber incorporation can be ascribed to disruption of S–I–S morphology. Figure 5 is the SEM photomicrograph of the S–I–S polymer, showing the morphology of the hard domains and the soft matrix, which, however, becomes disrupted on incorporation of the fiber, as shown in Figure 3.

Dynamic Storage Modulus

Figure 6 shows the plot of storage modulus vs. temperature plot of S–I–S composites filled with various loadings of carbon fiber. It was observed that below T_g the modulus increased sequentially with filler loading, but at higher temperature, the unfilled and 5 phr-filled composite have similar moduli. Increase in filler loading to 10 phr caused an increase in moduli, but at 20 phr fiber loading, the moduli increase was less marked. Below T_g, the hard and soft domains of the polymer cannot be differentiated and the effect of fiber on the modulus follows the pattern of the effect of fillers on a glassy polymer. The following relationship as depicted in Figure 7 between low-temperature dynamic modulus and filler loading was found to be obeyed:

$$E'_c = E'_m + KV_f \quad (1)$$

where E'_c and E'_m are the storage modulus of the composite and matrix, respectively, and K is the interaction parameter, the value of which is obtained from the slope of the plot of Figure 7. In this case, the value of K was found to be 1.863×10^0. A similar relationship has been found to exist in the case of carbon black-filled rubber vulcanizates.[16,17]

At temperatures above room temperature, nonsequential variation of the modulus with filler loading occurred, possibly due to disruption of the S–I–S morphology by incorporation of the fiber. Figure 8 shows the plot of the storage modulus at room temperature (25°C) against the volume fraction of the fiber. Here, also, a similar relationship [eq. (1)] was obtained but with a different K value of 3.56×10^7. This shows that the fiber–matrix interaction is less at room temperature than it is in the glassy state.

Dynamic Mechanical Damping

Figure 9 shows the plots of mechanical damping vs. temperature for the S–I–S copolymer filled with different loadings of carbon fiber. As observed from the figure, the tan δ_{max} peak at −48°C corresponds to the glass transition of the polyisoprene phase of the S–I–S matrix. The tan δ_{max} peak for the polystyrene phase could not be observed, as discussed earlier. Similar observations were also reported by other authors.[18] It is also evident that the tan δ_{max} in the glass-transition region decreased with incorporation of fiber into the matrix. It was also observed that fiber incorporation does not cause any shift in the glass transition temperature of the rubbery phase. This observation is similar to previous findings.[13,19,20] When tan δ values of the composites at T_g were plotted against the volume fraction of the filler (V_f), the following relationship, as depicted by Figure 10, was found to hold well:

$$(\tan \delta_{max})_c = (\tan \delta_{max})_m - \beta V_f \quad (2)$$

Table III Physical Properties of the Composites

Properties		Mix No. S_0	S_5	S_{10}	S_{20}
Modulus (MPa)					
10%	L[a]	0.25	0.25	0.51	0.59
	T[b]		0.25	0.35	0.62
25%	L	0.38	0.41	0.67	1.00
	T		0.41	0.60	1.15
50%	L	0.50	0.52	0.75	1.02
	T		0.51	0.70	1.10
Tensile strength (MPa)	L	15.70	12.40	11.70	4.40
	T		12.20	10.80	4.60
Elongation at break (%)	L	1670	2025	2050	1880
	T		2100	2100	1860
Tear strength (N/mm)	L	28.20	21.60	20.60	16.20
	T		20.30	19.90	15.00
Hardness (Shore A)		30	33	35	37

[a] Longitudinal.
[b] Transverse.

where $(\tan \delta_{max})_c$ and $(\tan \delta_{max})_m$ are the tan δ_{max} of the composite and matrix, respectively. β is the interaction parameter obtained from the slope of the plot in Figure 10. A similar observation has been reported by several workers.[21-23] The value of β in this case was found to be 11.71.

It was also observed from Figure 9 that there exists a temperature range from 0 to 70°C, where the tan δ does not change with temperature. But with the increase of fiber loading, tan δ values increased sequentially. Properties in this temperature region are important in the sense that the composites find applications in this range. Whereas in the glass transition region tan δ decreased on fiber incorporation, in the plateau region, tan δ increased on fiber incorporation. The variation of tan δ with fiber concentration, as shown in Figure 10, can be expressed in terms of the following equation:

$$(\tan \delta_{max})_c = (\tan \delta_{max})_m + \beta V_f \qquad (3)$$

where β is the interaction parameter dependent on

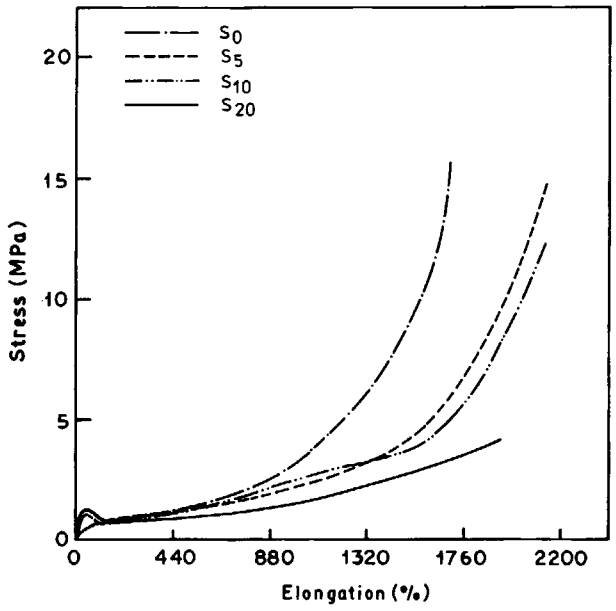

Figure 4 Stress–strain behavior of the filled and unfilled matrix.

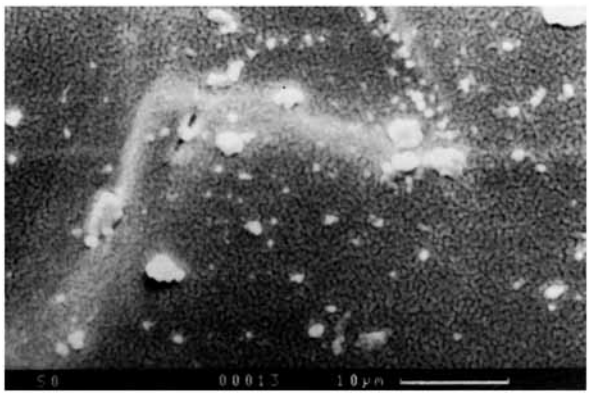

Figure 5 SEM photomicrograph of cryogenically fractured S–I–S matrix.

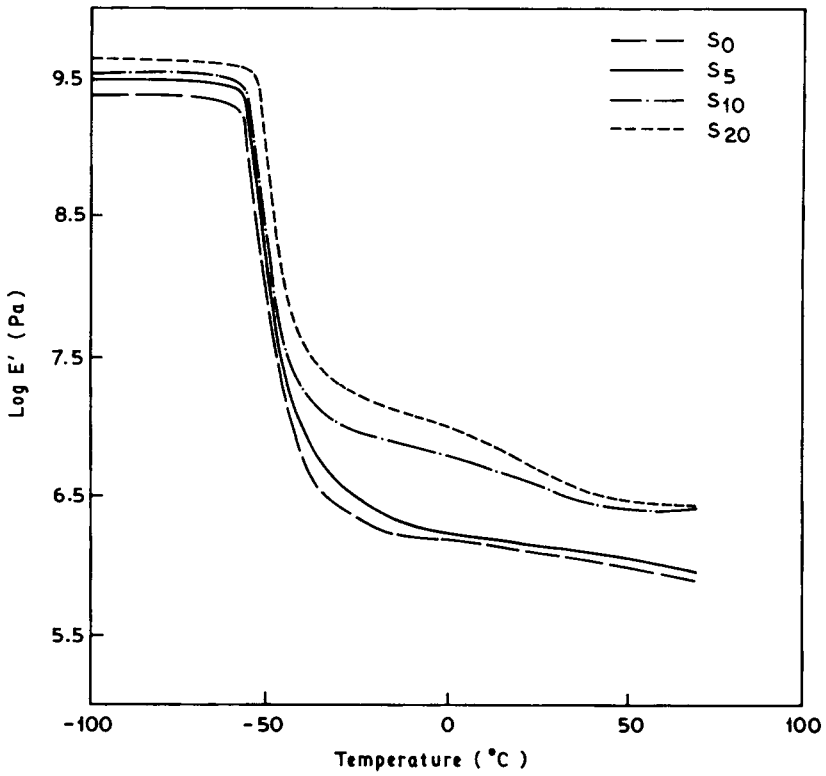

Figure 6 Variation of storage modulus with temperature for S–I–S composites at different fiber loadings.

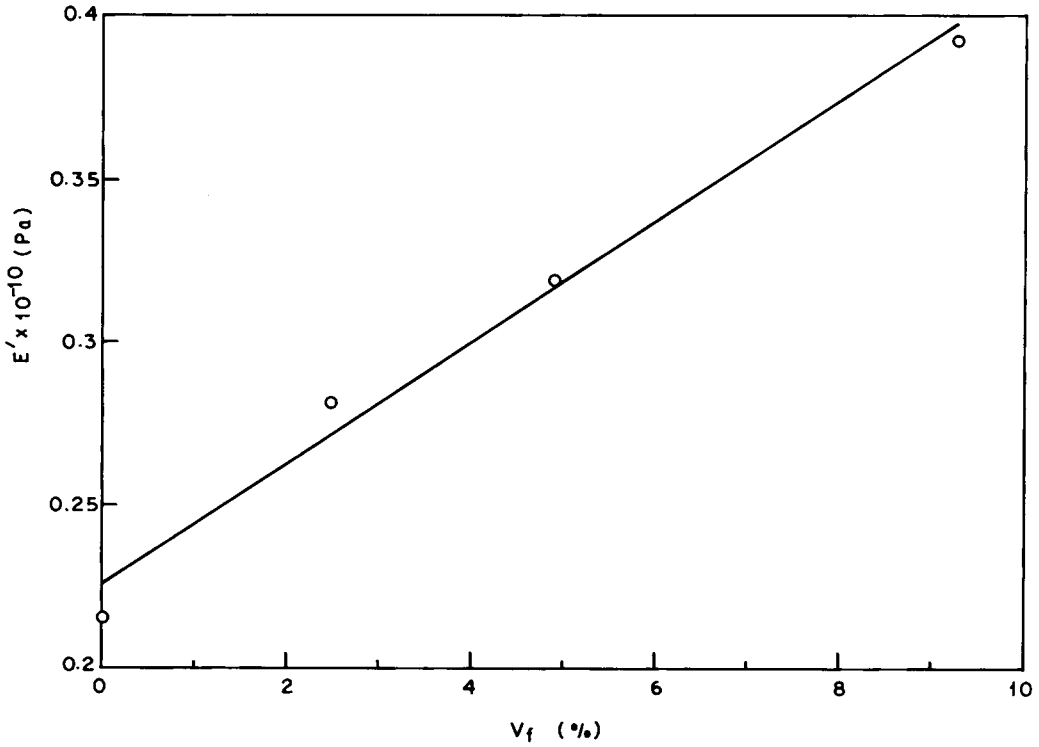

Figure 7 Effect of fiber loading (V_f) on storage modulus of the composites at the glass transition region (−60°C).

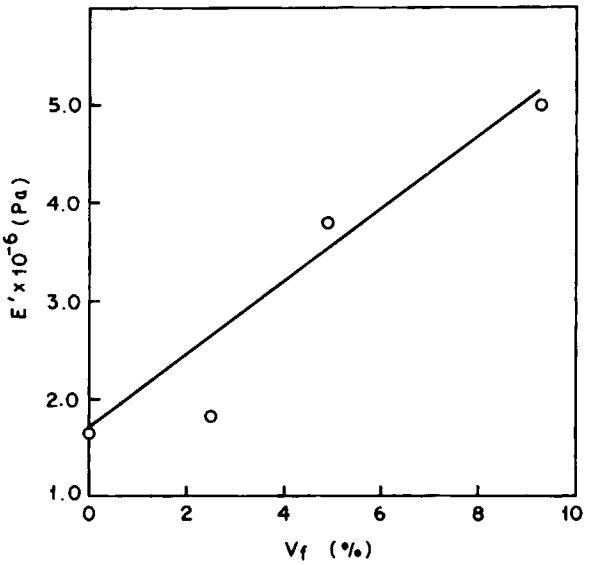

Figure 8 Effect of fiber loading (V_f) on storage modulus of the composites at room temperature (25°C).

the fiber matrix systems. The value of β in this case was found to be 3.14. The significance of β values [eqs. (2) and (3)] are similar to that of K values [eq. (1)] in the sense that the polymer–fiber interaction is higher in the glassy region than in the rubbery region (at room temperature).

Effect of Frequency

Figures 11 and 12 show the effect of applied frequency on the variation of storage modulus and mechanical damping with temperature, respectively. An increase in frequency caused an increase in modulus and the effect of frequency on the dynamic modulus was prominent at and above the T_g. An increase in frequency caused lowering of tan δ values at the glass transition region of the rubbery phase. But in the plateau region (0–70°C), an increase in frequency caused an increase in tan δ values. The effect of increasing frequency on dynamic modulus and damping results is a phenomenon that is similar to the effect of filler incorporation into the polymer. It is also apparent that the effect of filler on the dynamic mechanical properties of a fiber-filled composite can be realized by varying the frequency without altering the filler concentration. Higher frequency, however, caused a shift in the glass transition to higher temperature. Ashida and co-workers[22] obtained a 7°C shift to higher temperature with a 10-fold increase

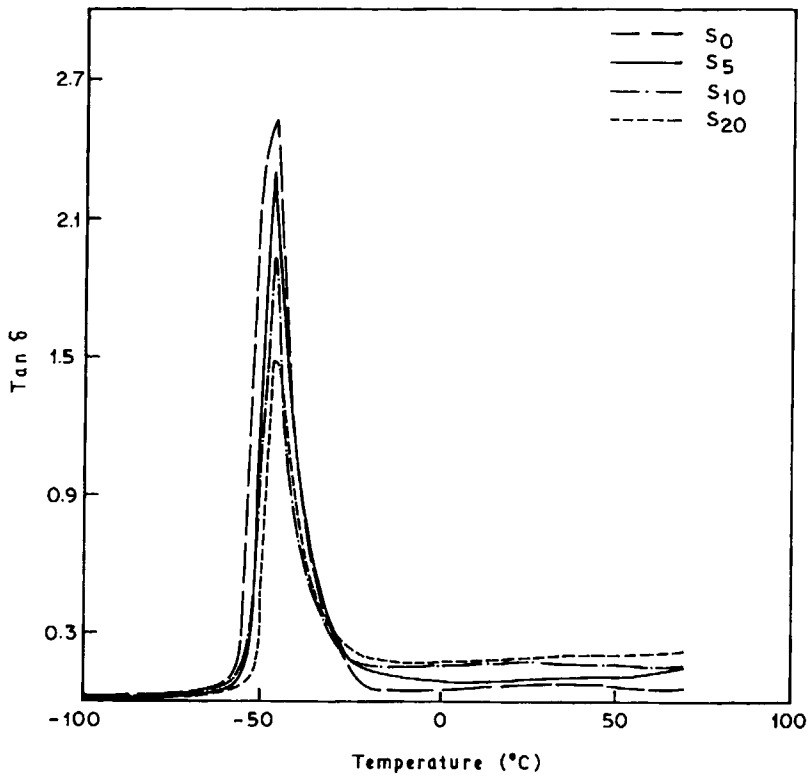

Figure 9 Variation of tan δ with temperature for the S–I–S composites at different fiber loadings.

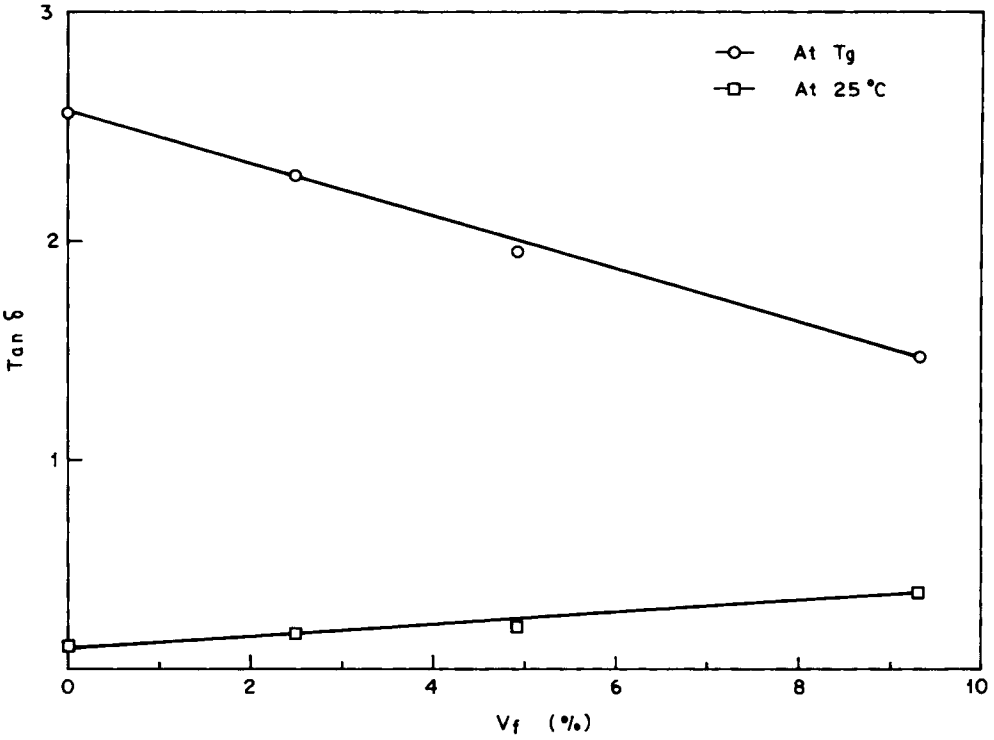

Figure 10 Effect of fiber loading on tan δ at glass transition temperature and at room temperature.

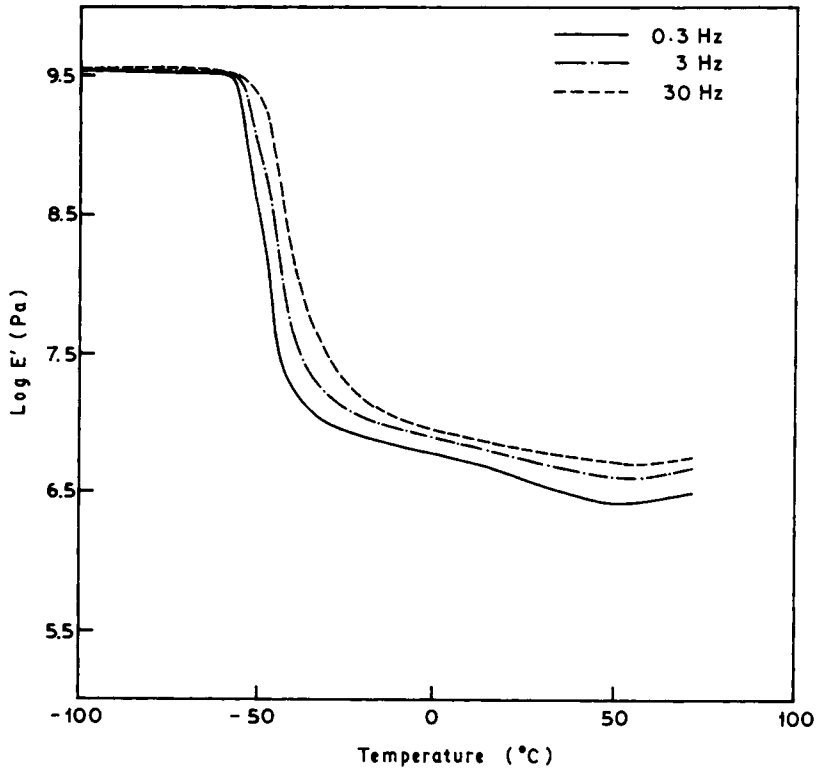

Figure 11 Effect of frequency on storage modulus with temperature for the S–I–S composite (S_{10}).

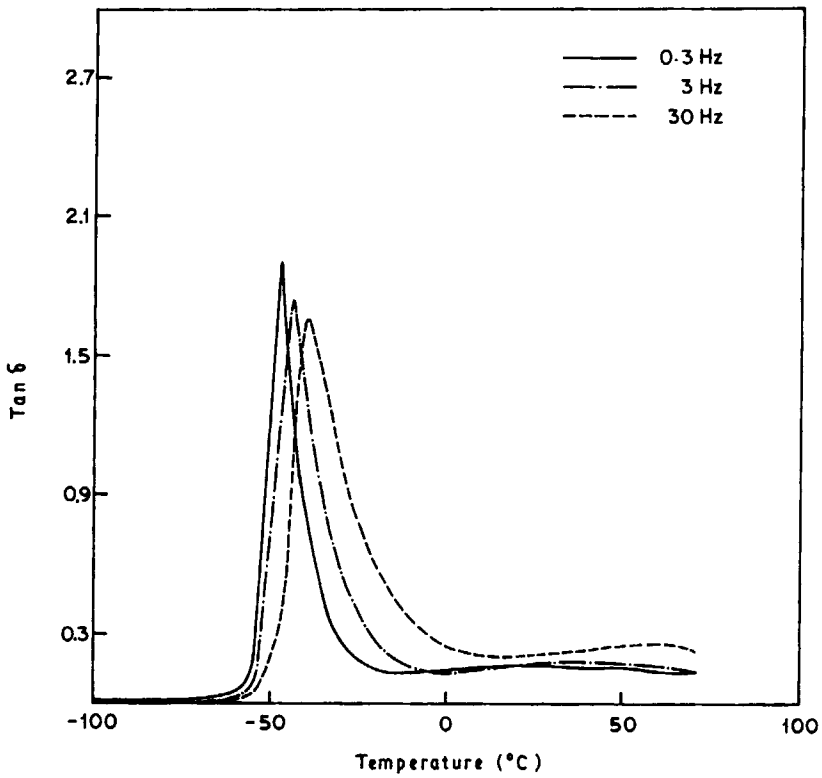

Figure 12 Effect of frequency on tan δ with temperature for the S–I–S composite (S_{10}).

of the frequency. The results of tan δ_{max} and T_g at different frequencies are tabulated in Table IV.

CONCLUSIONS

1. Brabender mixing of carbon fiber in S–I–S copolymer caused about a 30-fold decrease in the fiber aspect ratio.
2. Brabender mixing followed by milling caused randomness in the fiber orientation.
3. As the fiber content increased, low-strain static moduli and hardness increased, but tensile and tear strength dropped.
4. Tan δ_{max} at the Tg region decreased with increase in fiber loading, but the glass-transition temperature remains unaltered. At room temperature, however, tan δ increased with the fiber concentration.
5. The storage modulus increased with incorporation of fiber into the matrix and the effect was found to be prominent at higher temperature.
6. Although the glass transition temperature

Table IV T_g and Corresponding tan δ Values of the Composites at Different Frequencies

	Frequency (Hz)									
	0.3		1		3		10		30	
Mix. No.	tan δ_{max}	T_g (°C)	tan δ_{max}	T_g (°C)	tan δ_{max}	T_g (°C)	tan δ_{max}	T_g (°C)	tan δ_{max}	T_g (°C)
S_0	2.57	−47	2.54	−46	2.52	−44	2.47	−41	2.44	−38
S_5	2.24	−47	2.17	−45	2.05	−43	1.97	−41	1.92	−37
S_{10}	1.94	−46	1.87	−44	1.83	−42	1.79	−40	1.73	−37
S_{20}	1.51	−45	1.48	−44	1.42	−42	1.41	−40	1.39	−37

shifted to higher temperature with increase in the applied frequency, the variation in both storage moduli and tan δ values with frequency followed a pattern similar to the variation of these properties on incorporation of filler.

REFERENCES

1. M. J. Folkes, in *Short Fibre Reinforced Thermoplastics,* Research Studies Press, Wiley, Chichester, 1982.
2. H. Brody and I. M. Ward, *Polym. Eng. Sci.,* **11,** 139 (1971).
3. M. J. Carling and J. G. Williams, *Polym. Compos.,* **11,** 307 (1990).
4. M. M. Qayyum and J. R. White, *Polym. Compos.,* **11,** 24 (1990).
5. J. E. O'Connor, *Rubber Chem. Technol.,* **50,** 945 (1977).
6. S. K. Chakraborty, D. K. Setua, and S. K. De, *Rubber Chem. Technol.,* **55,** 1208 (1982).
7. V. M. Murty and S. K. De, *J. Appl. Polym. Sci.,* **29,** 1355 (1984).
8. L. A. Goettler, in *Handbook of Elastomers—New Developments and Technology,* A. K. Bhowmick and H. L. Stephens, Eds., Marcel Dekker, New York, 1988.
9. S. R. Moghe, *Rubber Chem. Technol.,* **49,** 1160 (1976).
10. S. Akhtar, P. P. De, and S. K. De, *J. Appl. Polym. Sci.,* **32,** 5123 (1986).
11. K. R. Watson and A. Frances, *Rubber World,* **198,** 20 (1988).
12. S. N. Kutty, P. P. De, and G. B. Nando, *Plast. Rubber Comp. Proc. Appl.,* **15,** 23 (1991).
13. D. Roy, A. K. Bhowmick, and S. K. De, *Polym. Eng. Sci.,* **32,** 971 (1992).
14. V. M. Murthy, S. K. De, S. S. Bhagawan, R. Sivaramkrishnan, and S. K. Athitan, *J. Appl. Polym. Sci.,* **28,** 3485 (1983).
15. S. K. De and V. M. Murthy, *Polym. Eng. Rev.,* **4,** 313 (1984).
16. A. I. Medalia, *Rubber Chem. Technol.,* **51,** 437 (1978).
17. L. E. Nielsen, *Mechanical Properties of Polymers and Composites,* Marcel Dekker, New York, 1974.
18. D. R. Saini, A. V. Shenoy, and V. M. Nadkarni, *J. Appl. Polym. Sci.,* **29,** 4123 (1984).
19. J. Ding, C. Chem, and X. Xue, *J. Appl. Polym. Sci.,* **42,** 1459 (1991).
20. M. Y. Boluk and H. P. Schreiber, *Polym. Comp.,* **7,** 295 (1986).
21. M. Ashida, T. Noguchi, and S. Mashimo, *J. Appl. Polym. Sci.,* **29,** 661 (1984).
22. M. Ashida, T. Noguchi, and S. Mashimo, *J. Appl. Polym. Sci.,* **30,** 1011 (1985).
23. L. Ibarra and C. Chamorro, *J. Appl. Polym. Sci.,* **37,** 1197 (1989).

Received February 11, 1992
Accepted August 4, 1992